# LINEAR AND NONLINEAR BEHAVIORS ON A SOIL SITE USING LOTUNG DOWNHOLE ARRAY IN TAIWAN

**H C HUANG[1], C S SHIEH[2] And H C CHIU[3]**


## SUMMARY

We study the linear and nonlinear behaviors of soft soil layers using DHB downhole recordings at LSST site, Lotung, Taiwan. This array includes five triaxial accelerometers deployed at depths of 0m, 6m, 11m, 17m and 47m. During a 6-year operation from 1985 to 1990, 30 earthquakes ($4.0 \leq M_L \leq 6.5$) triggered this array. The maximum PGA value is 257 gals recorded at the surface station. Spectral analyses show that the strong motion causes the peaks of ratio to shift to lower predominant frequencies. The averaged spectral ratio of 15 well-recorded weak motion records are selected as a reference, the shift of the maximum predominant frequency can reach 20%. Comparing to the weak motions, the strong motions also decrease the amplification factor. The maximum reduction of the amplification can reach 50%. Besides, the results of waveform simulation show that the linear model based on the Haskell method can well predict the weak motions (PGA < 60 gals) at various depths. However, this linear model does not work for the strong motion data (PGA > 150 gals). Here the nonlinear numerical scheme, such as DESRA-2, is required and can significantly improve the simulation results although the PGA value at the surface station is still underestimated. Overall, it is feasible to predict the strong motions for a horizontal layered structure.


## INTRODUCTION

Linear and nonlinear site effects have been examined in several studies [e.g., Joyner and Chen, 1975; Yu et al., 1993; Aguirre and Irikura, 1995, 1997] recently. Basically, the amplification of the seismic waves originates from the strong contrast between the physical properties of the rocks and the sediments. To evaluate this amplification, the seismic response of the soil is treated as a linear behavior under low levels of strain. But for larger stress-strain levels, the soil testing results at the laboratory showed a nonlinear relation which represents the nonlinear character of the soil response. Some authors have been trying to find the observational evidences of the nonlinearity from seismological data and estimate how much it influences strong ground motions [Chin and Aki, 1991; Beresnev et al., 1995a; Aguirre and Irikura, 1995, 1997]. The nonlinear effect caused the reduction of waveform amplitude in the time domain and shifts to lower frequencies and peak reduction in the frequency domain, because of the nonlinear response of the material that causes change in the elastic properties of the medium dependent on the waveform amplitudes. Aguirre and Irikura (1997) studied the nonlinearity, liquefaction, and velocity variation of soft soil layers in Port Island, Kobe, during the 1995 Hyogo-ken Nanbu earthquake. The S-wave velocity structure before and after the mainshock was found to be different. Specifically, the S-wave velocity of the second layer (5m to 16m depths) after the mainshock was 20% lower than before. Besides, the liquefied state remains at least 3 hr after the mainshock but no more than 24 hr. The strong influence of nonlinearity during the mainshock yielded a big reduction (25%) of the horizontal surface ground motions.

Several techniques have been used to detect the nonlinear effect. One is to evaluate spectral ratio of the observed data between the surface and bedrock during weak and strong ground motions [Ordas and Faccioli, 1994; Beresnev et al., 1995a]. Another option for estimating the soil layers effect is to use data from a vertical array of


[1] *Institute of Applied Geophysics, National Chung Cheng University, Chia-Yi, Taiwan, R.O.C.,Email: seihuey@eq.ccu.edu.tw*
[2] *Institute of Earth Science, Academia Sinica, Taipei, Taiwan R.O.C., Email: chiu@earth.sinica.edu.tw*
[3] *Institute of Earth Science, Academia Sinica, Taipei, Taiwan R.O.C., Email: chiu@earth.sinica.edu.tw*

seismometers [Wen et al., 1994, 1995; Beresnev et al., 1995b; Satoh et al., 1995]. The reduction and / or shift of the peaks during strong motion are an indication of the nonlinearity. Another technique used to evaluate nonlinearity is based on the comparison of the observed ground motions during strong motion with those simulated by a linear method. Two commonly used linear methods are the empirical Green's function and the 1D Haskell method. Numerical approaches to predict the nonlinear response of soil can be classified as either an equivalent secant approach [e.g. the SHAKE program by Schnabel et al. (1972)] or a direct nonlinear approach [e.g. the DESRA2 program by Lee and Finn (1978) and the CHARSOIL program by Streeter et al. (1974)]. Yu et al. (1993) used a direct nonlinear approach, DESRA2, to examine the differences between linear and nonlinear soil response with various levels of base excitations. They showed that in strong excitations soil nonlinear causes deamplification and also a shift in peak frequencies to lower values for an unsaturated shallow soil deposit of 20m thickness. Ni et al. (1997) used a modified version of DESRA2 constitutive model for saturated soil to study the nonlinear seismic response including liquefaction of medium dense soil deposits of various depths. The results of the stress-dependent soil properties model show lower deamplification and higher first-mode (resonant) frequency than that of the stress-independent soil properties model.

In this article, the Lotung vertical array data are used to study the linear and nonlinear behavior of soft soil layers. First, we calculate the spectral ratio by dividing the spectrum at surface relative to that at the depths of 6m, 11m, 17m, and 47m for the strong motion and weak motion events. In order to investigate the physical properties, two numerical schemes based on a horizontal layered structure model are used to simulate the 20 May 1986 earthquake sequence including the foreshock, aftershock and mainshock events. Besides, the nonlinear numerical schedule, DESRA-2, is also used to predict the ground accelerations of the strong motion events.

## SITE AND DATA

The downhole array is in the Lanyang alluvial deposits at the LSST (Lotung large-Scale Seismic Test) site in the southwest quadrant of the SMART1 array, Lotung in northeastern Taiwan (Figure 1). The sediments are mostly composed of interlayered silty sand and silty clay bed with gravel. [Anderson and Tang, 1989]. This site is geotechnically classified as "deep cohesionless soil site". This vertical array is composed of five triaxial accelerometers deployed at the depths of 0m, 6m, 11m, 17m and 47m. Digital data were recorded as 12-bit words at the rate of 200 samples per second. During a 6-year operation from 1985 to 1990, 30 earthquakes ($4.0 \leq M_L \leq 6.5$) triggered this array. The relative epicentral locations for these earthquakes are also shown in Figure 1. The maximum PGA value is 257 gals recorded at the surface station. Here events with peak ground acceleration at surface larger than 150 gals are attributed to the "strong motion" and less than 50 gals are considered as the "weak motion". The rough classification to quantify earthquake is the same as defined in Wen et al. (1995).

On the spectral ratio analysis, a 5 to 10-sec window, primarily bracketing the large amplitude S-wave parts of seismograms, is used with a 5% cosine taper. We choose the 10-sec window for the strong motion and the 5-sec window for the weak motion. The Fourier amplitudes are calculated for all accelerograms used. In order to avoid the pseudo-peak, twenty consecutive smoothing using a 3-point running Hanning average is applied to the raw spectra and then spectral ratios are computed. For all the waveforms used, the signal-noise ratios are so high that errors in the spectrums introduced by the noise is insignificant.

## SPECTRAL ANALYSIS

We calculate spectral ratios at surface relative to the depths of 6m, 11m, 17m and 47m. Figure 2 shows the RMS results during the May 20, 1986 earthquake sequence (No. 6, 7 and 8). The thin, thick and dot-thin lines individually represent the foreshock (No. 6), mainshock (No. 7) and aftershock event (No. 8) of this earthquake sequence. Compared with foreshock (4.5Hz, 3.0Hz, 2.2Hz and 1.3Hz) and aftershock (4.2Hz, 2.9Hz, 2.2Hz and 1.2Hz), mainshock event (2.8Hz, 1.7Hz, 1.2Hz and 0.85Hz) apparently has lower fundamental predominant frequency and amplification factor. Four frequencies in the parentheses represent the fundamental predominant frequency at the depths of 6m, 11m, 17m and 47m for that event. Many researchers attribute the phenomenon to the nonlinear behavior of soft soil. Besides, for the aftershock event, in 12 minutes after mainshock, the soil property is recovering but the predominant frequency at the first soil layer is still lower than the foreshock. It probably can be explained that the return time (12 minutes) of the soft soil is too short to go back to the initial state and then aftershock follows closely. For the furthermore investigations, 15 weak motion events are chosen.

Figure 3 shows the comparisons between the mainshock (thin line) and the average of the 15 weak motion events (thick line) at surface taken by four different depths. For the weak motions, the fundamental frequency at 0m/6m, 0m/11m, 0m/17m and 0m/47m individually appears at about 4.9Hz, 3.0Hz, 2.2Hz and 1.2Hz. When the frequency band is less than 10Hz, the strong motion event has lower fundamental predominant frequency than the weak motion events at the various depths. The largest shifting between them is about 20%. The amplification factor also decreases about 50% for the strong motion event. When the frequency range is between 10 and 20 Hz, the amplification factor of the strong motion becomes higher than the weak motion. These two lines intersect at about 10Hz. The above results are similar to Wen et al. (1994, 1995). Yu et al. (1993) also got the similar results using the theoretical simulation. It indicates that the strong motion event induces the nonlinear behavior of soil at LSST array. Besides, the same results also appear in the other 3 strong motion events (No. 4, 12 and 17).

## NUMERICAL SIMULATIONS

We divide the numerical simulations into two parts. One is based on the 1D Haskell method for the linear model. Another one is for the nonlinear model, that is, the DESRA-2 numerical scheme.

### Linear Model

The Lotung downhole array is located at the Lanyang alluvial plain. The shallow soil structure at this area can be approached to a horizontal layered structure [Wen and Yeh, 1984]. In order to study site amplification, we use the Haskell method [Haskell, 1953, 1960, 1962; Huang and Chiu, 1996] to simulate the ground motion of the horizontal and layered structure at the Lotung downhole site. The ground motion at the surface site is chosen as the input to predict those at the depths of 6m, 11m, 17m and 47m. The great advantage of this approach is that the upgoing (or direct S) wave need not be separated from the downgoing (or reflected) wave. By means of this technique, the whole waveform corresponding to each layer can be calculated directly. The used velocity structure and density are listed in Table 1 [Wen, 1994]. No attenuation term (1/Qs=0) is added to the simulation process. This is because the effect of Qs values is small; it is assumed to be negligible here.

In this part, the recordings of the 20 May 1986 earthquake sequences at the Lotung downhole site are analyzed. According to the back-azimuths of the earthquakes, two horizontal components are used to construct the SH wave. The velocity structure is divided into 11 layers and is considered to be at the half-space under the 47m depth. It is assumed that the SH wave is vertically incident from the half-space and the ground motion at surface site is used to predict those at downholes. Figure 4 shows the synthetic results (thick lines) compared with the observed data (thin lines) for the 8 April 1986 earthquake (No. 6). The synthetic waveforms at the depths of 6m, 11m, 17m and 47m can match the observed one well in amplitude and in phase. According to more simulation works, the simplified model gives a good result for weak ground motions (PGA < 60 gals) although they are not shown here. However, for the aftershock event (No. 8), the synthetic waveforms match the observed one neither in amplitude nor in phase (Figure 5(a)). This indicates that the velocity at shallow depths needs to be examined more thoroughly. The fundamental resonance frequency of a layer is $f = v_s / 4H$, where $v_s$ is the S-wave velocity and $H$ is the layer thickness. According to the formula, we can estimate the predominant frequency for the horizontal layered model. Therefore, a modified velocity structure is reconstructed. That is the S-wave velocity at the first layer is adjusted from 120 to 95 m/sec. Figure 5(b) shows the synthetic waveforms for the modified velocity structure. Evidently, both fit better in amplitude and in phase. But for the mainshock event (No. 7), the original velocity model (Table 1) can not afford the simulation of the strong motion event (Figure 6). Especially at the depth of 47m, the synthetic result is bad. However, the result can not be improved by means of adjusting velocity structure or incident angle. It means that the linear model based on Haskell method does not work well for the strong ground accelerations (PGA > 150 gals). This phenomenon is probably caused by the nonlinear effect of the soft soil after strong motion. In order to solve the problem, the nonlinear numerical schedule, such as DESRA-2, will be used to predict the strong ground accelerations.

### Nonlinear Model

To examine the DESRA-2 numerical schedule, we do the tests but not shown here and get the same results with Yu et al. (1993). The velocity structures and relative input parameters are listed in Table 2 where $G_{\max} = \rho v_s^2$, $\tau_{\max} = 0.0005 G_{\max}$, and b value is relative to 5% damping ratio [Yu et al., 1993; Ni et al., 1997]. First, the recording at the depth of 47m is selected to be the input motion to predict the ground motion at surface and other depths. Figure 7(a) shows the synthetic results (thick lines) compared with the observed data (thin lines) for the

20 May 1986 mainshock event (No. 7). The amplitude at surface is underestimated about a factor of 0.5, but they still have good fits in phase. It indicates that some problems appear in the velocity structure or the nonlinear behavior probably happens in the shallower structure after strong motion. Therefore, we change the recording at the depth of 17m as the input motion. The simulated result is shown in Figure 7(b). Apparently, there are better agreements in both amplitude and phase. The stress-strain relationship and stress variation with time at the depth of 10m are shown in Figure 8. Before 10 seconds, the strain value is small and the stress-strain relationship approaches a linear ("A" part in Figure 8(a)). As the strain becomes higher, the stress-strain relationship follows the Masing curve ("$B_1$" and "$B_2$" part). The "C" point is where the maximum stress and the maximum strain happen at about 10 seconds. After that, the strain decreases again, the stress-strain relationship also turns to be a linear trend ("D" part). According to the above discussions, the soil has produced evident strain changes during the mainshock event. Therefore, the nonlinear numerical scheme, DESRA-2, is required and can significantly improve the simulation results although the PGA value at the surface station is still underestimated. Overall, it is feasible to predict the strong motions for a horizontal layered structure.

## CONCLUSION

In order to study the linear and nonlinear behavior of the soft soil layers, the ground accelerations of a DHB vertical array at LSST site in Lotung is analyzed here. There are 30 earthquakes detected by this array during a 6-year operation. The maximum PGA value is 257 gals recorded at the surface station. Spectral analyses show that the strong motion (PGA > 150 gals) causes the peaks of ratio to shift to lower predominant frequencies. The averaged spectral ratio of 15 well-recorded weak motion records (PGA < 60 gals) are selected as a reference, the shift of the maximum predominant frequency can reach 20%. Comparing to the weak motions, the strong motions also decrease the amplification factor. The maximum reduction of the amplification can reach 50%. Besides, the results of waveform simulation show that the linear model based on the Haskell method can well predict the weak motions at various depths. However, this linear model does not work well for the strong motion. In this paper, the nonlinear numerical scheme, DESRA-2, is required and can significantly improve the simulation results although the PGA value at the surface station is still underestimated. Overall, it is feasible to predict the strong motions for a horizontal layered structure.

## REFERENCES


Aguirre, J. and K. Irikura (1995), "Preliminary analysis of nonlinear site effects at Port Island vertical array station during the 1995 Hyogoken-Nanbu Earthquake", *J. Natural Disaster Science*, 16, pp49-58.

Aguirre, J. and K. Irikura (1997), "Nonlinearity, liquefaction, and velocity variation of soft soil layers in Port Island, Kobe, during the Hyogoken-Nanbu Earthquake", *Bull. Seism. Soc. Am.* , 87, pp1244-1258.

Anderson, D.G. and Y.K. Tang (1989), "Summary of soil characterization program for the Lotung large-scale seismic experiment", Proc. EPRI/NRC/TPC workshop on seismic soil – structure interaction analysis technique using data from Lotung, Taiwan, Electric Power Research Institute, Palo Alto, CA, Vol. 1, pp4-1 – 4-20.

Beresnev, I.A., K.L. Wen, and Y.T. Yeh (1995a), "Nonlinear soil amplification: its corroboration in Taiwan", *Bull. Seism. Soc. Am.*, 85, pp496-515.

Beresnev, I.A., K.L. Wen, and Y.T. Yeh (1995b), "Seismological evidence for nonlinear elastic ground behavior during large earthquakes", *Soil Dyn. Earthquake Eng.*, 14, pp103-114.

Chin, B.H. and K. Aki (1991), "Simultaneous study of the source, path, and site effects on strong ground motion during the 1989 Loma Prieta earthquake: a preliminary result on pervasive nonlinear site effects", *Bull. Seism. Soc. Am.*, 81, pp1859-1884.

Haskell, N. A. (1953), "The dispersion of surface waves on multilayered media", *Bull. Seism. Soc. Am.,*, 43, pp17-35.

Haskell, N. A. (1960), "Crustal reflection of plane SH waves", *J. Geophys. Res.*, 65, pp4147-4150.

Haskell, N. A. (1962), "Crustal reflection of plane P and SV waves", *J. Geophys. Res.*, 67, pp4751-4767.

Huang, H.C. and H.C. Chiu (1996), "Estimation of site amplification from Dahan downhole recordings", *Earthquake Eng. Struct. Dyn.*, 25, pp319-332.

Joyner, W. B. and A. T. F. Chen (1975), "Calculation of nonlinear ground response in earthquake", *Bull. Seism. Soc. Am.*, 65, pp1315-1336.

Lee, M. K. W. and W. D. L. Finn (1978), "Dynamic effect stress response analysis of soil deposits with energy transmitting boundary including assessment of liquefaction potential", Rev., Dept. of Civil Eng., Soil Mechanics Series No. 38, the Univ. of British Columbia, Vancouver, Canada.

Ni, S. D., R. Siddharthan and J. G. Anderson (1997), "Characteristics of nonlinear response of deep saturated soil deposits", *Bull. Seism.. Soc. Am.*, 87, pp342-355.

Ordas, M. and E. Faccioli (1994), "Site response analysis in the valley of Mexico: selection of input motion and extent of nonlinear soil behavior", *Earthquake Eng. Struct. Dyn.*, 23, pp895-908.

Satoh, T., T. Sato, and H. Kawase (1995), "Nonlinear behavior of soil sediments identified by using borehole records observed at Ashigara Valley, Japan", *Bull. Seism. Soc. Am.*, 85, pp1821-1834.

Schnabel, P. B., Lysmer, J., and Seed, H. B. (1972), "SHAKE: a computer program for earthquake response analysis of horizontally layered sites", *Report EERC* 72-12, Earthquake Engineering Research Center, University of California, Berkeley.

Streeter, V.L., E.B. Wylie, and F.E. Richart (1974), "Soil motion computation by characteristic method", *J. Geotech. Eng. Div. ASCE* , 100, pp247-263.

Wen, K.L. and Y.T. Yeh (1984), "Seismic velocity structure beneath the SMART1 array", *Bull. Inst. Earth Sci. Acad. Sin.*, 4, pp51-72.

Wen, K. L. (1994), "Nonlinear soil response in ground motion", *Earthquake Eng. Struct. Dyn*., 23, pp599-608.

Wen, K. L., I. A. Beresnev, and Y. T. Yeh (1994), "Nonlinear soil amplification inferred from downhole strong seismic motion data", *Geophys. Res. Lett.*, 21, pp2625-2628.

Wen, K. L., I. A. Beresnev, and Y. T. Yeh (1995), "Investigation of nonlinear site amplification at two downhole strong ground motion arrays in Taiwan", *Earthquake Eng. Struc. Dyn.*, 24, pp313-324.

Yu, G., J. G. Anderson, and R. Siddharthan (1993), "On the characteristics of nonlinear soil response", *Bull. Seism. Soc. Am*., 83, pp218-244.

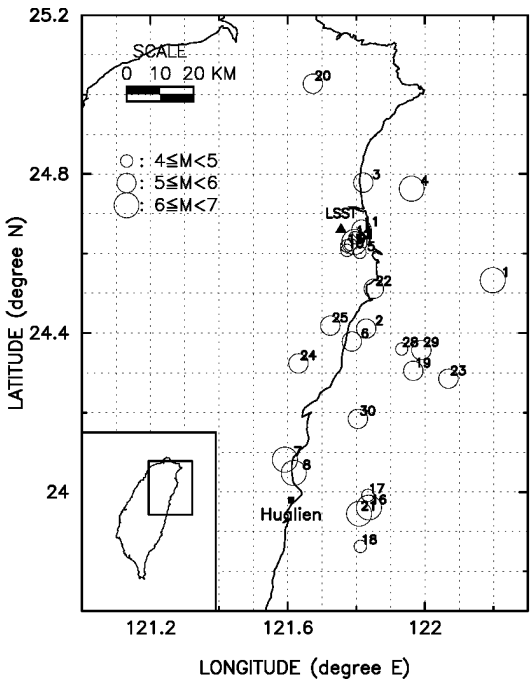


**Figure 1. The epicenters of 30 earthquakes ($4.0 \le M_L \le 6.5$) triggered the Lotung downhole array at the LSST site during a 6-year operation from 1985 to 1990.**

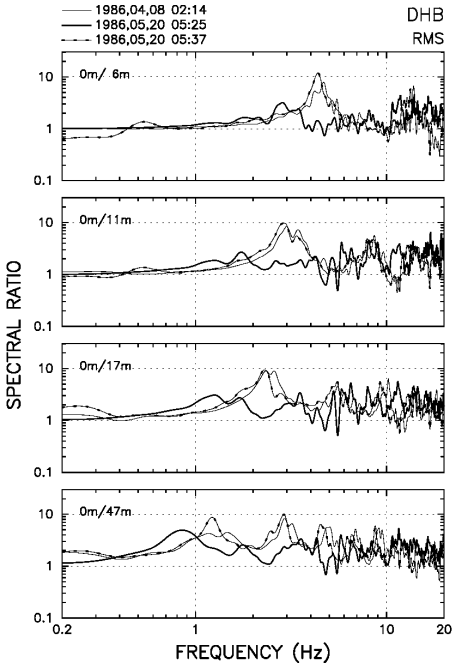


**Figure 2. The RMS spectral ratios at surface relative to the depths of 6, 11, 17 and 47m for the May 20, 1986 earthquake sequence. The thin, thick and dot-thin lines individually represent the foreshock (No. 6), mainshock (No. 7) and aftershock events (No. 8) .**

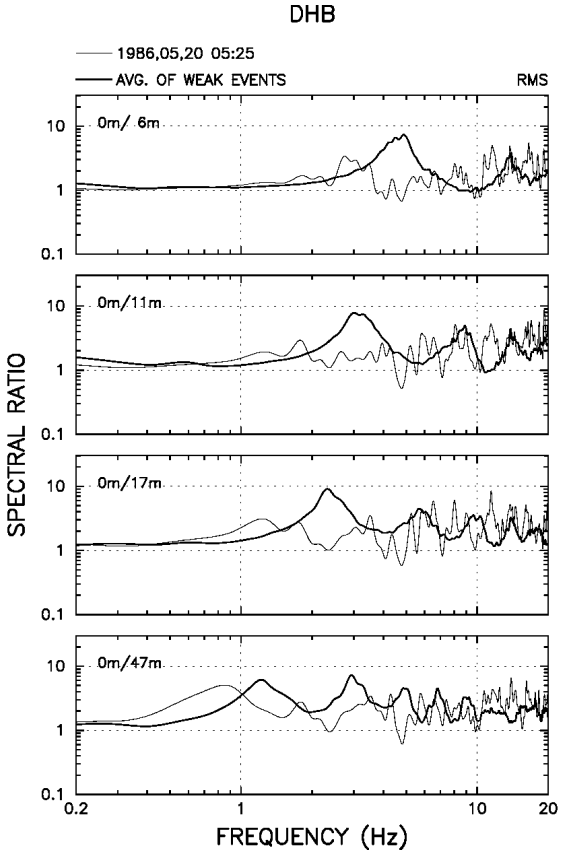


**Figure 3. Comparisons between the 20 May 1986 mainshock (thin line) and the average of the 15 weak motion events (thick line) at surface taken by four different depths.**

**Table 1. Velocity structure used in Haskell method at the Lotung downhole array**

| Layer No. | Thickness (m) | $V_P$ (m/sec) | $V_s$ (m/sec) | Density (g/cm$^3$) |
|---|---|---|---|---|
| 1 | 3 | 370 | 120 | 1.87 |
| 2 | 2 | 370 | 120 | 1.87 |
| 3 | 1 | 810 | 140 | 1.87 |
| 4 | 2 | 810 | 140 | 1.87 |
| 5 | 3 | 1270 | 190 | 1.87 |
| 6 | 2 | 1270 | 190 | 1.87 |
| 7 | 4 | 1330 | 220 | 1.87 |
| 8 | 7 | 1330 | 220 | 1.87 |
| 9 | 7 | 1330 | 220 | 1.87 |
| 10 | 3 | 1330 | 280 | 1.90 |
| 11 | 13 | 1250 | 250 | 1.90 |

**Table 2. Velocity structure used in DESRA-2 scheme at the Lotung downhole array**

| Layer no. | Thickness (m) | $V_s$ (m/sec) | Density (g/cm$^3$) | $G_{max}$ (MPa) | $\tau_{max}$ (KPa) | b values |
|---|---|---|---|---|---|---|
| 1 | 5 | 120 | 1.87 | 26.93 | 13.46 | 0.0027 |
| 2 | 3 | 140 | 1.87 | 36.65 | 18.33 | 0.0014 |
| 3 | 5 | 190 | 1.87 | 67.51 | 33.75 | 0.0017 |
| 4 | 18 | 220 | 1.87 | 90.51 | 45.25 | 0.0052 |
| 5 | 3 | 280 | 1.90 | 148.96 | 74.48 | 0.0007 |
| 6 | 13 | 250 | 1.90 | 118.75 | 59.38 | 0.0033 |

Note • (1) b value represents about 5% damping ratio.
(2) 1 Pa=1 N/m2

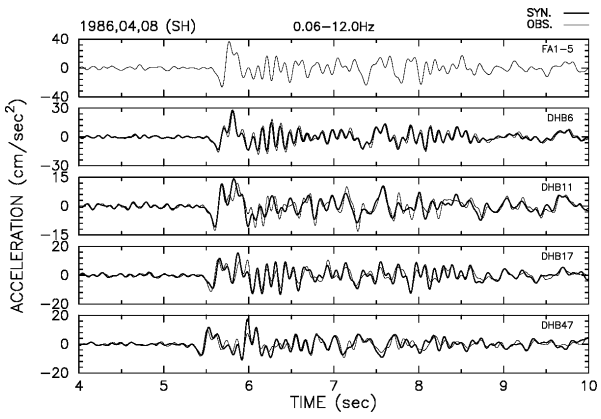


**Figure 4. The synthetic ground acceleration (thick line), using Haskell method, compared with the observed data (thin line) at the Lotung downhole site in the 8 April 1986 earthquake (No. 6). The recording at surface is selected as the input motion.**

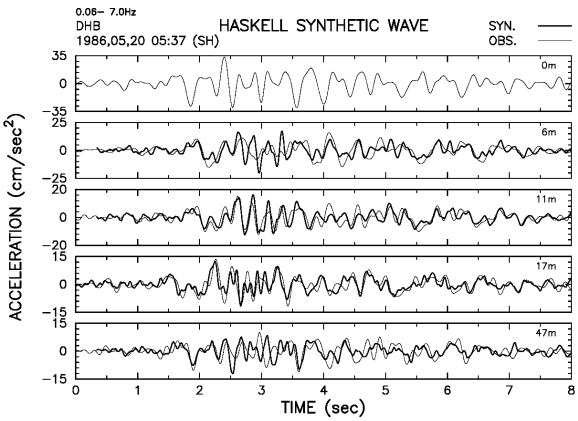


**Figure 5(a). The synthetic ground acceleration (thick line), using Haskell method with the velocity model in Table 1, compared with the observed data (thin line) at the Lotung downhole site in the 20 May 1986 aftershock event (No. 8). The recording at surface is selected as the input motion.**

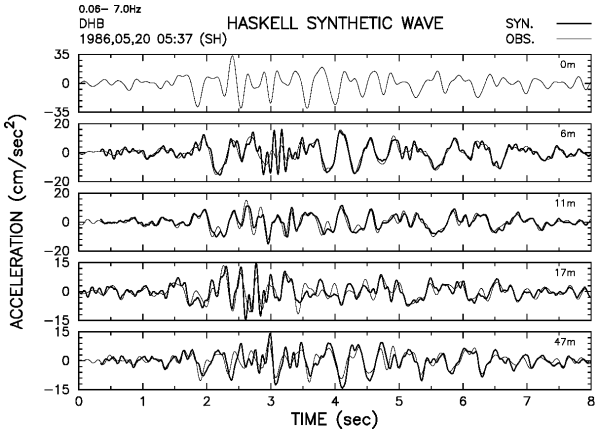


**Figure 5(b). The synthetic ground acceleration (thick line), using Haskell method with the modified velocity model (the velocity of the first layer is changed from 120 to 95 m/sec), compared with the observed data (thin line) at the Lotung downhole site in the 20 May 1986 aftershock event (No. 8). The recording at surface is selected as the input motion.**

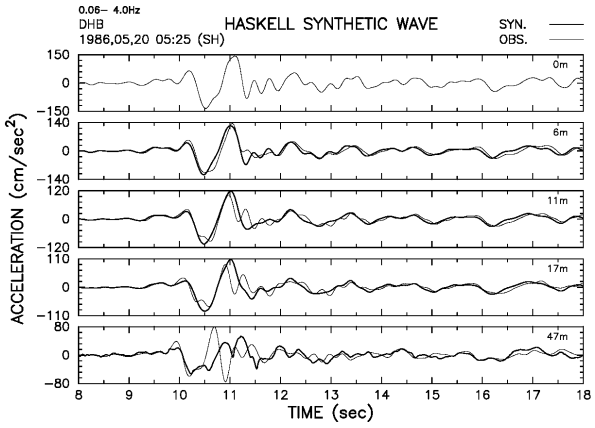


**Figure 6. The synthetic ground acceleration (thick lines), using Haskell method, compared with the observed data (thin lines) at the Lotung downhole site in the 20 May 1986 mainshock event (No. 7). The recording at surface is selected as the input motion.**

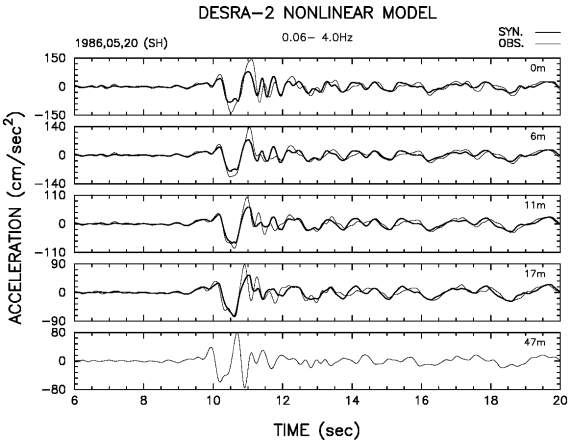


**Figure 7(a). The synthetic ground acceleration (thick lines), using DESRA-2 numerical schedule, compared with the observed data (thin lines) at the Lotung downhole site in the 20 May 1986 mainshock event (No. 7). The recording at the 47m depth is selected as the input motion.**

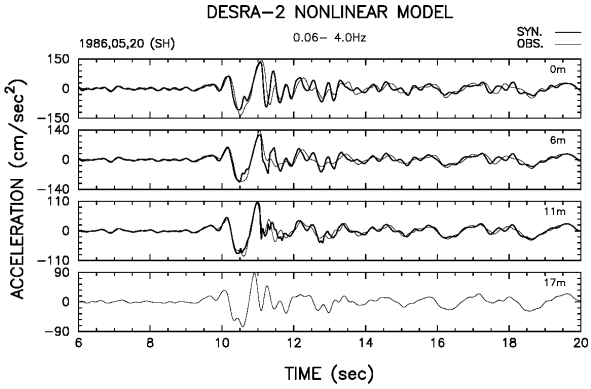


**Figure 7(b). The synthetic ground acceleration (thick lines), using DESRA-2 numerical schedule, compared with the observed data (thin lines) at the Lotung downhole site in the 20 May 1986 mainshock event (No. 7). The recording at the 17m depth is selected as the input motion.**

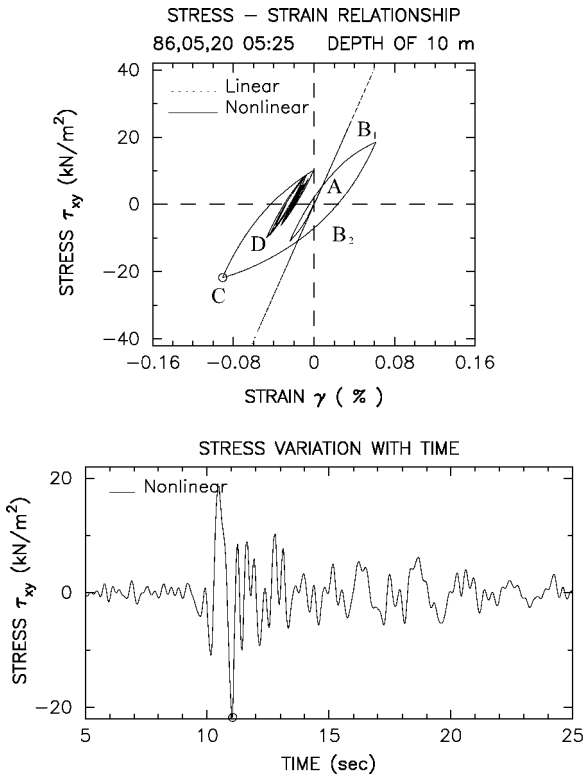


**Figure 8. The stress-strain relationship (a) and stress variation with time (b) at the 10m depth of the Lotung downhole site in the 20 May 1986 mainshock event (No. 7).**